

Carbon fibres with ordered graphitic-like aggregate structures from a regenerated cellulose fibre precursor

A.E. Lewandowska*, C. Soutis**, L. Savage***, S.J. Eichhorn*

* College of Engineering, Maths & Physical Sciences, Physics Building, University of Exeter, Stocker Road, Exeter, EX4 4QL, UK;

Email: s.j.eichhorn@exeter.ac.uk.

** Aerospace Research Institute, University of Manchester, Faculty of Engineering & Physical Sciences, Manchester M13 9PL, Lancashire, UK

*** College of Engineering, Mathematics and Physical Sciences, University of Exeter, North Park Road, EX4 4QF, Exeter, UK.

Abstract The production and characterisation of low modulus carbon fibres is reported from a commercially available regenerated cellulose fibre (Cordenka™). The fibres were heat treated before the graphitisation at a temperature of 200 °C. Fibres were further heat treated and graphitised at a temperature of 2000 °C. Polarised Raman spectra of carbonised/graphitised fibres were recorded. The ratio of two Raman peaks located at $\sim 1350\text{ cm}^{-1}$ (D-band) and at $\sim 1600\text{ cm}^{-1}$ (2D band) – the I_D/I_G ratio – were used to follow the onset and development of the carbon/graphitic structure. It is shown that single carbon fibres processed at 2000 °C have a modulus of $\sim 70\text{ GPa}$ and strain at break $>2\%$. A Raman spectroscopic method that follows the shift in the position of the 2D band suggests a modulus of $\sim 77\text{ GPa}$. Transmission Electron Microscope imaging of the fibres reveals a sub-structure containing aggregates of oriented concentric turbostratic carbon domains, some of which are reminiscent of carbon nanotubes. These relatively high strength fibres (1.5 GPa) could be possible alternatives to E-glass fibres in low weight ($\sim 30\%$ lighter than E-glass), high volume automotive and marine applications. It is also shown that these fibres can be converted in a woven precursor form to a carbon fibre fabric without the need to weave brittle filaments.

Keywords: A. Carbon fibres; B. Strength; C. Deformation; D. Raman spectroscopy

1. Introduction Carbon fibres are entirely based on the element carbon and represent some of the lightest inorganic materials available for industrial application. Their use has dominated the recent surge in the development of lightweight composite materials, particularly for use in aerospace applications *e.g.* Boeing's 787 Dreamliner [1]. The use of carbon fibres for composite materials is set to grow dramatically over the next 5-10 years, with high volume market applications in the automotive sector being predicted to be one such growth area. Polyacrylonitrile (PAN) has been traditionally used as a precursor for high modulus/strength carbon fibres [2]. Before the development of PAN based carbon fibres, cellulose was used by Union Carbide in the 1950s to make mid-range modulus materials [3,4]. Production of carbon fibres using PAN is known to produce toxic gases *e.g.* hydrogen cyanide, whose extraction during the process increases costs [5]; not an issue for cellulose precursors. There has recently been a resurgence of interest in the use of more sustainable and environmentally friendly precursor materials for the production of carbon fibres, particularly for medium stiffness and strength. Cellulose fibres lend themselves very well for this purpose [6], with continuous filaments being produced in an established industrial process and in large volumes for applications in the textile and tyre cord industries. Much progress has been made in the intervening years from the 1950s to develop highly oriented cellulose fibres, which could serve as much better precursors for carbon fibres. One such example are Cordenka fibres, the use of which for this purpose, is the topic of the present work.

Cordenka fibres are produced using a viscose process, with the addition of formaldehyde, forming a derivative of cellulose in sodium hydroxide, which is subsequently dissolved in carbon disulphide and converted back to cellulose using dilute sulphuric acid [7]. High stiffness fibres are produced, whose properties have been reported by a number of authors [8,9]. Their conversion to carbon fibres has not been previously reported, and neither their conversion from a woven form. Recent work has shown that both a liquid crystalline cellulose precursor and lyocell can be converted to carbon fibres

with moduli >100 GPa [10]. In the present work, the microstructure and micromechanics of graphitised Cordenka fibres and woven fabrics using Raman spectroscopy are reported.

The technique of Raman spectroscopy has been used to identify and characterise various forms of graphitic structures [11,12] and to better understand the structure-mechanical properties of carbon fibres [13-17]. Typically the Raman spectrum of carbon fibres contains three main features; the G band (located at $\sim 1600\text{ cm}^{-1}$), the D-band (at $\sim 1350\text{ cm}^{-1}$) and the 2D (or G') band (at $\sim 2660\text{ cm}^{-1}$) [12,17]. The ratio of the intensities (I_D/I_G) can be used to give an indication of the level of graphitization of the material. It has been shown that both the G and 2D bands shift in position under the application of external tensile deformation [18]. Most notably it has been shown that the magnitude of the 2D band shift rate with respect to strain is directly proportional to the fibre modulus [15]; the same is true for the G band shift rate [19]. This approach allows one to predict the modulus of a carbon fibre based on a simple measurement of the shift rate with respect to strain of a single filament in air. The approach has previously been reported for Bocell fibres (a liquid crystalline spun cellulose fibre), and here now for Cordenka, a commercially available cellulose fibre that is widely used as a tire cord yarn, and which can be woven in a fabric form, has also been reported as a potential composite reinforcement [20-23].

2. Experimental

2.1. Materials The precursor fibre used for the preparation of carbon filaments was Cordenka-700. This is a commercial regenerated cellulose fibre with a linear density between of 2440 dtex. The specified mechanical properties for this fibre are: breaking force 96.1 - 184.6 N, breaking tenacity 510 - 483 mN tex⁻¹. In addition a plane weave fabric using the same fibres was supplied by Cordenka GmbH. The fabric type was MA 1, 1220 dtex, T0 with a weight of 295 g m⁻².

2.2. Pretreatment of cellulose fibres The pre-treatment (or stabilisation) process of the fibres was carried out in an Elite 2216CC tube furnace (Elite Thermal System Limited). The fibres were first cut into short bundles and placed in a ceramic boat. Prior to the heating, the tube was purged with nitrogen for 30 min to remove air and to stabilise the nitrogen flow. Fibres and fabrics were initially pre-treated

by heating to 200 °C in nitrogen at a rate of 2 °C min⁻¹, followed by a 30-min isotherm at the final maximum temperature.

2.3. Carbonisation and graphitisation of cellulose fibres and fabrics Cordenka-700 fibres and woven fabrics were first cut into 50 mm bundles (50×50 mm fabrics) and placed in a graphitic furnace insert separated by graphite sheets. Prior to the heating, the chamber was pressurised under vacuum for 5 min to remove air, which was maintained until 900 °C. The process of carbonisation and graphitisation of the fibres was performed according to the following procedure: Fibres were initially pre-treated by heating to 240 °C in a vacuum at a rate of 5 °C min⁻¹, followed by a 30 min isotherm at the final maximum temperature. The sample was carbonised by heating up to 900 °C in a vacuum, then up to 1500 °C in an argon atmosphere at a rate of 10 °C min⁻¹, again followed by a 30-min isotherm at the final maximum temperature. In the case of the carbonisation process at 2000 °C, the heating rate amounted to 10 °C min⁻¹ up to 1700 °C and subsequently to 2000 °C at a rate of 5 °C min⁻¹, followed by a 30-min isotherm at the final maximum temperature. The processes were carried out in a HPW25 hot press furnace (FCT System GmbH). Cordenka-700 fibres carbonised at 400, 600, 800, 1000, 1500 and 2000 °C are labelled as Cordenka 700-400, Cordenka 700-600, Cordenka 700-800, Cordenka 700-1000, Cordenka 700-1500 and Cordenka 700-2000- respectively. Woven fabrics were placed in a graphite 'box/coffin' and was initially stabilised by heating in a coke dust environment. The material was stabilised by heating to 200 °C at a rate of 2 °C min⁻¹, followed by a 90-min isotherm at the final maximum temperature. Graphitisation of the stabilised textile was performed in a resistance heated furnace (called a “Holman Tube”). The long sidewalls of the furnace were connected to the electrodes and act as the resistance heating elements. The furnace was at set 2950 °C at the start of the hold and by the end of the 1.5 - 2.0 hrs hold the temp was 3060 - 3085 °C.

2.5. Electron Microscopy of Fibres The morphology of pure and carbonised Cordenka-700 fibres were studied using a HITACHI S3200N SEM-EDS scanning electron microscope operated at an acceleration voltage of 5 kV. Prior to the imaging, the fibres were fixed on metal stubs using carbon tape and sputter-coated at ~20 mA with a thin layer of gold. To perform transmission electron

microscopy (TEM) of carbonised fibre samples were embedded in a low-viscosity epoxy resin (SpurrTM). The embedded bundles were cut using a diamond knife into slices of ~100 nm thickness. The fibre bundle axis was oriented perpendicular to the cutting plane. The slices were deposited onto 400 mesh TEM copper grids (holey carbon films) and investigated using a JEM-2100 LaB6 TEM operated at 200 kV in a bright field mode. The magnifications used for the collection of SEM images were 1000× and 2000×, while for TEM images 400,000× was used.

2.6. Polarised Raman spectroscopy Orientation of the cellulose chains and graphite planes along the fibre axis were studied using Raman spectroscopy. The measurements were performed using a Renishaw RM-1000 System equipped with a thermoelectrically cooled CCD detector. The laser was focused on the samples using a Leica microscope with a ×50 objective lens. For the cellulose fibres, a 785 nm wavelength laser was used to record spectra using an exposure time of 10 s and three accumulations. The power of the laser was reduced to 50 % of the source power. The incident and scattered laser light were polarised parallel to the principal axis of the spectrometer. This polarisation configuration is denoted "VV". The Cordenka 700 fibres' axes were oriented parallel to the polarisation configuration of the laser light used to excite and record the Raman scattering. A half-wave plate was used to rotate the polarisation direction for incident light, while a polariser/analyser was used to maintain the polarisation direction of scattered light parallel to the principal axis of the spectrometer. The incident laser light was rotated from 0 to 180° and each Raman spectrum was recorded at 4° increments. The intensity of a Raman band located at ~1090 cm⁻¹ was used for the orientation studies of the cellulose. This band was fitted using a Lorentzian function. Intensities outputted from this fitting procedure were normalised to a Raman band localised at ~1262cm⁻¹ (which does not change in intensity with rotation of the sample). This approach allowed two polarisation arrangements; first where the incident and scattered light are parallel to the principal axis of the spectrometer ("VV" configuration) and second where the polarisation of incident light is rotated by 90° by the half-wave plate ("HV" configuration).

For the carbon fibres, a 532 nm wavelength laser was used to record Raman spectra using an exposure time of 10 s and five accumulations. The power of laser was reduced to 1 % of the source power to avoid heating effects. The fibres' axes were oriented parallel to the polarisation configuration of the laser light. The incident laser light was rotated from 0 to 180° using a half-wave plate and each Raman spectrum was recorded at 5° increments. The D, G and 2D Raman bands were used for the carbon fibre orientation studies and were fitted using a Lorentzian function. The intensities were all normalized for a maximum intensity of unity.

2.7. Raman spectroscopy of carbonised and graphitised fibres The laser coupled to the Renishaw RM-1000 spectrometer was focused on the pyrolysed fibre samples using a ×50 objective lens. A 532 nm wavelength laser was used to collect Raman spectra from the carbonised/graphitised filaments. The power of laser was reduced to 1 % of the source power to minimise an overheating of the samples. Single spectra were recorded with an acquisition time consisting of five accumulations of 10 s. The fibre bundle axis was oriented parallel to the polarisation direction of the laser light used to excite and record the Raman scattering. The fabrics were characterised using a WITec confocal Raman microscope system coupled to a 514 nm laser. The D and G Raman bands were fitted using a Lorentzian function in the wavenumber range 2100-650 cm^{-1} and to 4 peaks.

To perform micromechanical studies on the fibres, single carbonised filaments were mounted onto a cardboard frame; the window in this card had a gauge length of 10 mm. The card was then inserted into an in-situ tensile and compression stage (Deben Microtest, 200N or 20N load cell). This was then placed under the Raman microscope so that the fibre axis was oriented parallel to the polarisation configuration of the incident and scattered laser light. The fibre was deformed in strain steps of 0.05% with a motor speed of 0.1 mm min^{-1} . Raman spectra were recorded at each strain increment using an exposure time of 60 s and one accumulation. The 2D Raman band was fitted using a Lorentzian function to find its position as a function of tensile deformation. From load and elongation data extracted from the tensile testing device, stress and strain were derived (for 5 samples). Cross-

sectional area of the fibres were determined individually by imaging the ends using SEM and the solid area calculated using ImageJ.

3. Results and discussion

3.1. Structural characterisation of cellulose fibres Figure 1 shows the Raman spectra obtained for Cordenka-700 fibres using "VV" and "HV" polarisation configurations. The spectrum obtained for a "VV" polarisation configuration is typically dominated by two intense and well resolved Raman bands located at $\sim 895\text{ cm}^{-1}$ and $\sim 1090\text{ cm}^{-1}$. The band located at 895 cm^{-1} is assigned to the C-O-C in plane stretching [24], while the band centred at 1090 cm^{-1} corresponds to C-O ring stretching modes and the β -1,4 glycosidic linkage (C-O-C) stretching modes between the glucose rings of the cellulose chains [24,25]. The intensity of the Raman bands assigned to the bond vibrations corresponding to the main chain segmental stretching and bending modes are sensitive to the orientation of the fibre with respect to the polarisation configuration. The direction in which the maximum change in polarizability occurs is related to the direction of the vibrational displacements. These changes are related to the directional character of the vibrational modes, their orientation and structure, which is a reflection of the arrangement of cellulose chains relative to the fibre axis [26,27].

The intense and well resolved Raman band centred at $\sim 1090\text{ cm}^{-1}$ associated with the C-O stretching modes within the cellulose molecule is useful for studying the orientation of the chains along the fibre axis. A degree of alignment of cellulose chains along the fibre length can influence a degree of alignment of carbon layers along the fibre axis. Figure 2 illustrates the changes in the normalised intensity of the band located at $\sim 1090\text{ cm}^{-1}$ as a function of the angle between the polarisation of incident laser direction and the axis of the Cordenka 700 fibre. A maximum intensity of this Raman band is obtained when the direction of the laser polarisation is parallel to the axis of the fibre and thus parallel to the cellulose molecules within the fibrils. The intensity of the Raman band at $\sim 1090\text{ cm}^{-1}$ gradually decreases when the direction of the laser polarisation is rotated to a direction perpendicular to the fibre axis. The intensity ratio of the band at 90° to the band at 0° (I_{90°/I_{0°) describes a degree of alignment of cellulose chains along the fibre axis. The value of I_{90°/I_{0° is low; 0.19 for Cordenka-700.

This suggests that fibre exhibits a high degree of alignment of cellulose chains along the fibre length, as has been reported for other highly oriented cellulose fibres such as flax [28] making it a potentially good precursor for highly oriented carbon fibres. It is also shown that these intensity data reported in Figure 2 can be fitted with a function of the form.

$$y = r + t \cos^4 \theta \quad (1)$$

where y is the intensity, θ is the angle and r and t are the fitting parameters. This form of curve has been previously reported for the fitting of orientation data for a graphene oxide nanocomposite [29].

3.2. Morphology of cellulose and carbon fibres and fabrics Cordenka-700 cellulose fibres exhibit a uniform diameter along their length. Additionally, the fibres show serrations typical of some viscose-like cellulose fibres [30] along the fibre axis as reported in Figure 3 (see Supplementary Information, Figure 1S for a low magnification). The surface of cellulose fibres is observed to be rough with the sizable flaws located near serrations. Typical images of the filaments carbonised/graphitised in the range 1000-2000 °C are shown in Figure 3b-d. The carbon fibres retain their morphology and the uniform diameter along their length after the carbonisation/graphitization process [10,31,32]. Also, the serrations along the fibre axis are present after processing. Fibres carbonised at a temperature of 1000 °C exhibit a rough surface with 'blisters' present (Fig. 3b). These 'blisters' are associated with a thermal degradation of cellulose at a lower temperature. The carbon fibres' surfaces become smoother with an increase in the carbonisation temperature. Random flaws are still distinguishable on the surface of the fibres carbonised at 1500 °C (Fig. 3c). Fibres graphitised at 2000 °C however have a smooth surface without visible defects, which is consistent with Bocell-based carbon fibres [10]. They still however retain the serrations along the fibre axis characteristic for the Cordenka-700 cellulosic precursor (Fig. 3d). Carbonised fabrics were found to shrink in size, but yet could be formed into a curved shape within the furnace (Fig. 4). The shrinkage, but particularly the distortion of the fabrics, can be mitigated by the use of a stabilisation step (see Supplementary Information, Figs 2S and 3S)

3.3. Formation of graphitic carbon nanostructures Typical TEM images of carbon fibre cross-sections shown in Figure 5 illustrate the formation of the graphitic carbon nanostructures during the

carbonisation/graphitisation process. Fibres carbonised at a temperature of 1000 °C consist of small and randomly oriented carbon-like structures embedded in an amorphous matrix (see Supplementary Information, Figure S4a). An increase in the carbonisation temperature to 1500 °C triggers the growth of ordered graphitic-like crystallites, which appear to be oriented with respect to each other (Fig. 5a). An average distance between the carbon layers obtained directly from the TEM images is estimated to be 0.348 nm. Larger crystallites with a preferred orientation appear after graphitisation at a temperature of 2000 °C (Fig. 5b and Supplementary Information, Figure S4b). A higher carbonisation temperature leads to a small decrease in the stacking distance of the carbon layers to 0.342 nm (although this may be within the error of the measurement itself). The values obtained for the plane spacing are larger than reported for graphite (0.335 nm) suggesting the formation of turbostratic carbon crystallites. The carbon layers formed after graphitisation at 2000 °C are arranged into quasi-cylindrical shapes, suggesting their preferred alignment along the fibre axis. The microstructure appears to comprise aggregates of such structures, which have remarkable similarities to cross-sections of multiwall carbon nanotubes. The formation of this structure is postulated to be via the graphitisation of the internal fibrillar structure of the regenerated cellulose fibres. Aggregate structures of carbon nanotubes forming fibres have been reported using top-down approaches [33], but not from a cellulose starting material via a "bottom-up" approach. The production of carbon nanotubes from cellulose-based precursors have also been reported in the literature [34-36]. It is possible therefore that this type of conversion has occurred although further work is required to confirm this.

3.4. Effectiveness of carbonisation/graphitisation process Raman spectroscopy of carbon fibres and fabrics was used to assess the effectiveness of the carbonisation/graphitisation process. The analysis of Raman spectra allows an estimation of the physical properties of the carbon fibres. However, it is necessary to point out that Raman spectroscopy effectively characterises the surface properties of fibres. Raman spectra of carbon fibres exhibit two sharp first-order Raman bands; the G band around 1580-1600 cm^{-1} is assigned to zone centre phonons of E_{2g} symmetry involving the in-plane bond-

stretching motion of pairs of C sp^2 atoms, whereas the D band centred around 1348 - 1370 cm^{-1} is related to a breathing mode of A_{1g} symmetry involving phonons near the K zone boundary [11,31,37]. At low carbonisation temperatures, the second-order 2D Raman band located at $\sim 2650\text{ }cm^{-1}$ is present as a broad peak from ~ 2400 to $\sim 3100\text{ }cm^{-1}$. The influence of the carbonisation temperature on the evolution of graphitic-like structures in the carbon fibres was studied using bundles of Cordenka 700 fibres. Figure 6 shows Raman spectra of the carbon fibres obtained at different carbonisation temperatures. These spectra exhibit two sharp first-order Raman bands independent of the carbonisation temperature. However, they become sharper and their relative intensity increases with an increase in the carbonisation temperature. Also, the second-order Raman bands undergo evolution. The 2D (G') Raman band evolves with an increase in temperature, exhibiting a small "bump" at low temperatures in the range of 600-1000 $^{\circ}C$, and later becoming more prominent at 2000 $^{\circ}C$. The appearance of the 2D Raman band at $\sim 2682\text{ }cm^{-1}$ for the fibres carbonised at 1500 $^{\circ}C$ indicates the possible onset of graphitisation [31]. Its development to the well-defined Raman band located at $\sim 2694\text{ }cm^{-1}$ further confirms the presence of turbostratic carbon structures visible in TEM images (*cf.* Fig. 5b) for the material carbonised at 2000 $^{\circ}C$.

Other features of the Raman spectrum can be used to describe a degree of graphitisation of carbon fibres, including the intensity ratio of the D band to the G band (the I_D/I_G ratio), the full width at half maximum (FWHM) intensity of the bands and the frequency of Raman bands [10,38,39]. According to previous research the magnitude of the I_D/I_G ratio has been correlated with the crystallite size of graphitic structures obtained from X-ray diffraction measurements [10-12,31,40]. The value of the I_D/I_G ratio increases with an increase in crystallite size up to 2.5 nm, whereas it typically decreases when the crystallite size is larger than 2.5 nm. Figure S5 illustrates the dependence of the I_D/I_G ratio on the carbonisation temperature. In the temperature range between 400 and 1500 $^{\circ}C$, the value of the I_D/I_G ratio increases with temperature, changing from 0.72 for Cordenka 700-400 to 1.25 for Cordenka 700-1500. This behaviour suggests an increase in the structural order in the fibres as has been reported for other cellulose fibres such as Bocell and electrospun cellulose nanofibres [10,31].

An increase in the carbonisation temperature to 2000 °C causes a decrease of the magnitude of the I_D/I_G ratio suggesting an increase of the graphitic-like crystallite size in the carbonised sample. This suggests that graphitisation of the sample has occurred. The I_D/I_G ratio of fibres graphitised at 2000 °C however exhibits variability for different measurement points along the bundle length. The spread in these data suggests that graphitisation is not uniform at this temperature, as detected at the surface of the fibres by Raman spectroscopy. Several points were scanned across a carbon fibre fabric (Fig. 7a). Typical Raman spectra obtained are shown in Figure 7b, indicating high values of the I_D/I_G ratio (>1 in most cases). Some variability is noted, which suggests that there is incomplete graphitization of the material. However, at a higher temperature ($>3000^\circ\text{C}$; Fig. S6) the I_D/I_G ratio drops significantly (≤ 0.2) which suggests a highly graphitized structure.

Polarized Raman spectroscopy was used to characterize the orientation of turbostratic carbon layers in the graphitised fibres. Figure 8 illustrates the variation of the normalised intensity of the D and 2D Raman bands as a function of the angle between the polarisation of incident laser direction and the axis of the Cordenka 700-2000 fibre. The changes in the intensity of the G band are significantly less pronounced than for the D and 2D bands (see Supplementary Information, Figure S7). These data in Figure 8 are also seen to follow Equation 1 (*cf.* Fig. 2). For both bands a maximum intensity is achieved when the direction of the incident laser polarisation is parallel to the Cordenka 700-2000 fibre axis and a minimum when it is perpendicular. A similar behaviour is described for the Raman band centred at $\sim 1090\text{ cm}^{-1}$ in the precursor material (*cf.* Fig. 2), for GO nanocomposites [30] and for functionalised multilayer graphene sheets [41]. The intensity ratio of the band at 90° to the band at 0° (I_{90°/I_{0°) describes a degree of alignment of carbon layers along the fibre axis. The value of I_{90°/I_{0° is 0.78 and 0.62 for the D and the 2D bands respectively. This suggests that the turbostratic carbon layers begin to align along the fibre axis with an increase in the graphitisation temperature; some misalignment is noted here which may lead to a lowering of mechanical properties. This feature is similar to the cellulose precursor (*cf.* Fig. 2) and confirms previous observations that carbon structures formed via carbonisation retain some "memory" of the starting structure [6].

3.5. Mechanical deformation studies of the graphitised fibres using Raman spectroscopy Figure 9a shows a typical SEM image of the morphology of a cross-section of a Cordenka fibre graphitised at a temperature of 2000 °C. This cross-section is serrated as was reported for images of the fibre lengths (cf. Fig. 3). A selected stress-strain curve for a fibre graphitised at 2000 °C is presented in Figure 9b. Mechanical deformation studies of carbon fibres obtained Young's modulus of 70.7 ± 2.4 GPa, a strength of 1.5 ± 0.2 GPa and a breaking strain of 2.2 ± 0.2 % (for n=5 tests). These values are slightly lower than those reported previously for carbon fibres obtained from electrospun cellulose nanofibres and Bocell [10,31] but similar to other rayon fibres [6]. Micromechanical studies are possible for carbon fibres with the presence of a well-resolved 2D Raman band; the position of this band is sensitive to deformation. This band has been reported towards a lower wavenumber position upon the application of tensile deformation applied to a number of carbon fibres, and carbon nanotubes [15,17,18,42]. The Cordenka 700-2000 sample shows an intense 2D Raman band located ~ 2690 cm^{-1} (Figure 6). Micromechanical studies were carried out using single fibres carbonised at 2000 °C. Figure 10a illustrates the shift in the 2D Raman band position upon tensile deformation. Figure 10b reports detailed shifts in the position of the 2D Raman band as a function of fibre axial strain. The rate of the shift in position of 2D Raman band was found to be -5 $\text{cm}^{-1}\%$ from a linear regression to these data. The fibre was found to break at a strain >1.9 %. To calculate the modulus of the fibres based on this shift rate we used a recent analysis derived by Androulidakis *et al.* [43]. For a fibre in air

$$\left[\frac{1}{\omega_{2D}} \right] \left(\frac{\Delta\omega_{2D}}{\varepsilon} \right)_{\text{air}} = - \left[\frac{\gamma_{2D}(1 - (\nu_{\theta\theta} + \nu_{rr}))}{E_g} \right] E_f \quad (2)$$

where ω_{2D} is the initial position of the 2D band, $(\Delta\omega_{2D}/\varepsilon)_{\text{air}} = -5$ $\text{cm}^{-1}\%$ (from the fit to the Raman data - see Fig. 10b), $\gamma_{2D} = 3.55$ [44], $\nu_{\theta\theta} + \nu_{rr} = 0.32$ [43] where $\nu_{\theta\theta}$ and ν_{rr} are the axial hoop and transverse Poisson's ratios, E_g is the Young's modulus of graphene (~ 1 TPa) and E_f is the fibre modulus. Fitting the 2D band position we obtained a value of $\omega_{2D} \sim 2691$ cm^{-1} . Using these values in equation 2 we obtain a fibre modulus $E_f \sim 77$ GPa, which is close to the value obtained by tensile

testing. A modulus of ~ 70 GPa begins to compete with other fibres e.g. E-glass. Given a typical density of carbon fibres of $1.8 \times 10^3 \text{ kg m}^{-3}$ and glass fibres of $2.5 \times 10^3 \text{ kg m}^{-3}$ yields specific moduli of $\sim 39 \text{ MNm kg}^{-1}$ (for the present carbon fibres using the tensile testing value of ~ 70 GPa) and $\sim 28 \text{ MNm kg}^{-1}$ (for E-glass, modulus = 70 GPa) [45]. This means that there is potential to make carbon fibres using these regenerated forms that can compete with glass for further use in applications where high volume production is required; glass fibres would be $\sim 30\%$ heavier but lower cost than carbon due to lower temperatures required during processing. The use of a sustainable, non-toxic and renewable precursor, such as cellulose, makes it more attractive than PAN. Improvement in the properties of the fibres could be achieved by the application of tension during carbonisation, or the use of hot stretching as has been recently demonstrated for rayon precursors [46]. Karacan and Gül [47] however applied tension on their viscose fibres (up to a temperature of $1000 \text{ }^\circ\text{C}$), but only achieved a modulus of ~ 36 GPa. The application of tension is important due to the presence of shrinkage during the carbonisation process, but even without this a tensile strength of ~ 1.5 GPa has been achieved in the present study. Future work will address the application of tension to improve the overall properties of the fibres.

4. Conclusions Commercial Cordenka 700 cellulose shows a comparable degree of alignment of the cellulose chains along the fibre axis compared to BocellTM; a high-modulus regenerated fibre. Transmission Electron microscopy of the fibre cross-sections reveals an interesting nanostructure of aggregated concentrically aligned turbostratic carbon layers, reminiscent of bundles of multiwalled carbon nanotubes. Raman spectroscopy has confirmed the progressive carbonisation of Cordenka 700 fibres, following the changes of intensities and positions of the D and G Raman bands. It is shown that carbon fibres, with a high degree of graphitization can be obtained by carbonisation of a woven fabric of Cordenka fibres. The increase in the structural order in the fibres with an increase of the carbonisation temperature is confirmed by the presence of a second-order 2D Raman band. Micromechanical tests of single carbon fibres reveal an estimated modulus of ~ 77 GPa and a failure strain $>2\%$. Discrepancy between this modulus value and one obtained via tensile testing (~ 70 GPa)

is thought to be due to the averaging of a highly graphitized skin and a less developed fibre core. This modulus and tensile strength of 1.5 GPa makes these fibres potentially competitive with E-glass fibres for high volume, relatively high performance applications e.g. automotive, marine and infrastructure. It was also shown that the cellulose fibres can be converted in a woven precursor and form to a carbon fibre fabric without the need to weave brittle filaments; further results will be reported in future publications.

Acknowledgements This work was supported by the Engineering and Physical Sciences Research Council [grant number: EP/IO33513/1], through the EPSRC Centre for Innovative Manufacturing in Composites (CIMComp). We would also like to thank Morgan Advanced Materials for their assistance with graphitization experiments.

References

- [1] Soutis C. Carbon fibre reinforced plastics in aircraft construction. *Mater Sci & Eng. A.* 2005; 412: 171-176.
- [2] Paris O, Peterlik H. The Structure of Carbon Fibres. In: Eichhorn SJ, Hearle JWS, Jaffe M, Kikutani T (eds) *Handbook of Textile Structure. Volume 2: Natural, regenerated, inorganic and specialist fibres.* 2009. Woodhead Publishing Ltd in Association with The Textile Institute, Manchester, UK.
- [3] Tang MM, Bacon R. Carbonization of cellulose fibers—I. Low temperature carbonisation. *Carbon.* 1964;2:211-220.
- [4] Bacon R, Tang MM. Carbonization of cellulose fibers 2. Physical property study. *Carbon* 1964;2 :221-225.
- [5] Chung DDL. 1994. *Carbon fibre composites.* Butterworth-Heinemann, Boston.
- [6] Dumanli AG, Windle AH. Carbon fibres from cellulosic precursors: a review. *J. Mater. Sci.* 2012; 47:4236-4250.
- [7] Woodings C (ed) .*Regenerated Cellulose Fibres.* 2001. Woodhead Publishing/The Textile Institute/CRC Press, Cambridge.
- [8] Eichhorn SJ, Sirichaisit J, Young RJ . Deformation mechanisms in cellulose fibres, paper and wood. *J. Mater. Sci.* 2001;36:3129-3135
- [9] Hajlane A, Kaddami H, Joffe R, Wallstrom L. Design and characterization of cellulose fibers with hierarchical structure for polymer reinforcement. *Cellulose* 2013;20:2765-2778.
- [10] Kong K, Deng L, Kinloch IA, Young RJ, Eichhorn SJ. Production of carbon fibres from a pyrolysed and graphitised liquid crystalline cellulose fibre precursor. *J Mater Sci* 2012;47:5402-5410.
- [11] Ferrari AC, Robertson J. Interpretation of Raman spectra of disordered and amorphous carbon. *Phys. Rev. B.* 2000;61:14095-14107.
- [12] Tuinstra F, Koenig JL. Raman spectrum of graphite. *J. Chem. Phys.* 1970;53:1126-1130.
- [13] Huang Y, Young RJ. Nonlinear elasticity in carbon-fibers. *J. Mater. Sci. Lett.* 1993;12:92-95
- [14] Huang YL, Young RJ. Structure-property relationships in carbon-fibers. *Inst. Phys. Conf. Ser.* 1993;130:319-322
- [15] Huang YL, Young RJ. Microstructure and mechanical-properties of pitch-based carbon-fibers. *J. Mater. Sci.* 1994;29:4027-4036

- [16] Young RJ, Andrews MC. Deformation micromechanics in high-performance polymer fibers and composites. *Mater. Sci. Engin. A*. 1994;184:197-205.
- [17] Cooper CA, Young RJ, Halsall M. Investigation into the deformation of carbon nanotubes and their composites through the use of Raman spectroscopy. *Compos. A Appl. Sci. Manuf.* 2001;32:401-411
- [18] Robinson IM, Zakikhani M, Day RJ, Young RJ, Galiotis C. Strain dependence of the Raman frequencies for different types of carbon-fibers. *J. Mater. Sci. Lett.* 1987;6:1212-1214.
- [19] Frank O, Tsoukleri G, Riaz I, Papagelis K, Parthenios J, Ferrari AC, Geim AK, Novoselov KS, Galiotis C. Development of a universal stress sensor for graphene and carbon fibres. *Nat. Commun.* 2011;2:255.
- [20] Graupner N, Beckmann F, Wilde F, Mussig J. Using synchrotron radiation-based micro-computer tomography (SR μ -CT) for the measurement of fibre orientations in cellulose fibre-reinforced polylactide (PLA) composites. *J. Mater. Sci.* 2014;49:450-460.
- [21] Meredith J, Coles SR, Powe R, Collings E, Cozien-Cazuc S, Weager B, Mussig J, Kirwan K. On the static and dynamic properties of flax and Cordenka epoxy composites. *Compos. Sci. Technol.* 2013;80:31-38.
- [22] Khan MA, Ganster J, Fink HP. Hybrid composites of jute and man-made cellulose fibers with polypropylene by injection moulding. *Compos. A*. 2009;40:846-851.
- [23] Savage L, Evans KE. The importance of the mesostructure in toughening cellulosic short fibre composites. *Compos. Sci. Technol.* 2014;93:97-105.
- [24] Edwards HGM, Farwell DW, Webster D. FT Raman microscopy of untreated natural plant fibres. *Spectrochim. Acta. A*. 1997;53:2383-2392.
- [25] Gierlinger N, Schwanninger M, Reinecke A, Burgert I. Molecular changes during tensile deformation of single wood fibers followed by Raman microscopy. *Biomacromol.* 2006;7:2077-2081.
- [26] Wiley JH, Atalla RH. Band assignments in the Raman-spectra of celluloses. *Carbohydr. Res.* 1987;160:113-129.
- [27] Tanpichai S, Quero F, Nogi M, Yano H, Young RJ, Lindstrom T, Sampson WW, Eichhorn SJ. Effective Young's modulus of bacterial and microfibrillated cellulose fibrils in fibrous networks. *Biomacromol.* 2012;13:1340-1349.
- [28] Bakri B, Eichhorn SJ. Elastic coils: deformation micromechanics of coir and celery fibres. *Cellulose* 2010;17:1-11.
- [29] Li ZL, Young RJ, Kinloch IA. Interfacial stress transfer in graphene oxide nanocomposites. *ACS Appl. Mater. Interf.* 2013;5:456-463.
- [30] Gordon Cook J, *Handbook of Textile Fibres: Man-Made Fibres*. 1984 (Merrow Publishing Co. Ltd, 5th Edn.).
- [31] Deng LB, Young RJ, Kinloch IA, Zhu YQ, Eichhorn SJ. Carbon nanofibres produced from electrospun cellulose nanofibres. *Carbon* 2013;58:66-75.
- [32] Arshad SN, Naraghi M, Chasiotis I. Strong carbon nanofibres from electrospun polyacrylonitrile. *Carbon* 2011;49:1710-1719.
- [33] Li YL, Kinloch IA, Windle AH. Direct spinning of carbon nanotube fibers from chemical vapor deposition synthesis. *Science* 2004;304:276-278.
- [34] Goodell B, Xie X, Qian Y, Daniel G, Peterson M, Jellison J. Carbon nanotubes produced from natural cellulosic materials. *J. Nanosci. Nanotech.* 2008;8:2472-2474.
- [35] Goodell BS, Xie X, Qian Y, Zhang D, Peterson ML, Jellison JL. Processes for producing carbon nanotubes and carbon nanotubes produced thereby. United States Patent 2011; US8080227 B1.
- [36] Dubrovina L, Naboka O, Ogenko V, Gatenholm P, Enoksson P. One-pot synthesis of carbon nanotubes from renewable resource: cellulose acetate. *J. Mater. Sci.* 2014;49:1144-1149.
- [37] Ferrari AC, Robertson J. Resonant Raman spectroscopy of disordered, amorphous, and diamondlike carbon. *Phys. Rev. B*. 2001;64:075414.

- [38] Larouche N, Stansfield BL. Classifying nanostructured carbons using graphitic indices derived from Raman spectra. *Carbon* 2010;48:620-629.
- [39] Nakamura K, Fujitsuka M, Kitajima M. Disorder-induced line broadening in 1st-order Raman-scattering from graphite. *Phys. Rev. B.* 1990;41:12260-12263.
- [40] Yoshida A, Kaburagi Y, Hishiyama Y. Full width at half maximum intensity of the G band in the first order Raman spectrum of carbon material as a parameter for graphitization. *Carbon* 2006;44:2333-2335.
- [41] Liang Q, Yao X, Wang W, Liu Y, Wong CP. A three-dimensional vertically aligned functionalized multilayer graphene architecture: an approach for graphene-based thermal interfacial materials. *ACS Nano.* 2011;5:2392-2401.
- [42] Lourie O, Wagner HD. Evaluation of Young's modulus of carbon nanotubes by micro-Raman spectroscopy. *J. Mater. Res.* 1998;13:2418-2422.
- [43] Androulidakis Ch, Tsoukleri G, Koutroumanis N, Gkikas G, Pappas P, Parthenios J, Papagelis K, Galiotis C. Experimentally derived axial stress-strain relations for two-dimensional materials such as monolayer graphene. *Carbon.* 2015;81:322-8.
- [44] Mohiuddin TMG, Lombardo A, Nair RR, Bonetti A, Savini G, Jalil R, et al. Uniaxial strain in graphene by Raman spectroscopy: G peak splitting, Gruneisen parameters, and sample orientation. *Physical Review B.* 2009;79(20).
- [45] Harris B. *Engineering Composite Materials.* 1999, IOM Communications Ltd., London.
- [46] Zhang X, Lu YG, Xiao H, Peterlik H. Effect of hot stretching graphitization on the structure and mechanical properties of rayon-based carbon fibers. *J. Mater. Sci.* 2014;49:673-684.
- [47] Karacan I, Gül A. Carbonization behavior of oxidized viscose rayon fibers in the presence of boric acid-phosphoric acid impregnation. *J. Mater. Sci.* 2014; 49; 7462-7475.

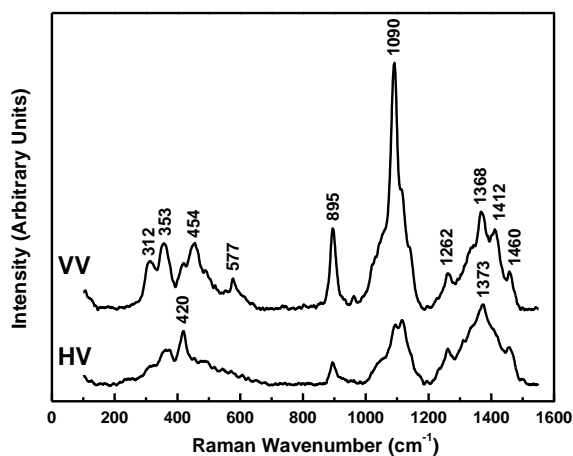


Fig. 1. Typical Raman spectra for Cordena 700 fibres obtained using "VV" and "HV" polarisation configurations. Some representative peak positions are marked on the spectra.

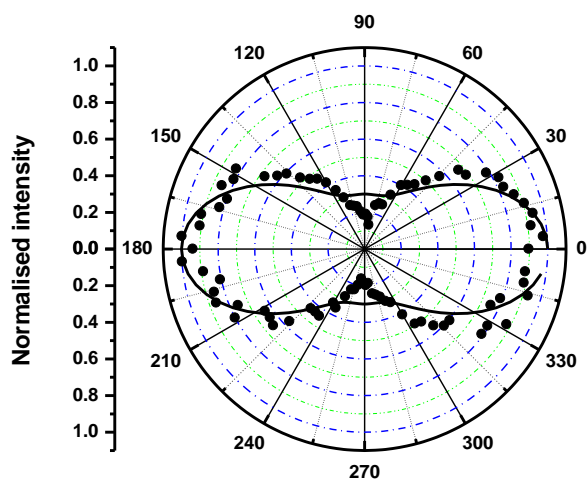


Fig. 2. Normalised intensity of the Raman band located at 1090 cm^{-1} as a function of the angle between the polarisation of incident laser direction and the axis of a Cordenka 700 cellulose fibre. Solid lines are fits to the data of the form $y = r + t\cos^4\theta$; $r = 0.2$ and $t = 0.8$ in (a) and $r = 0.3$ and $t = 0.7$ in (b). R^2 values for each fit are 0.9.

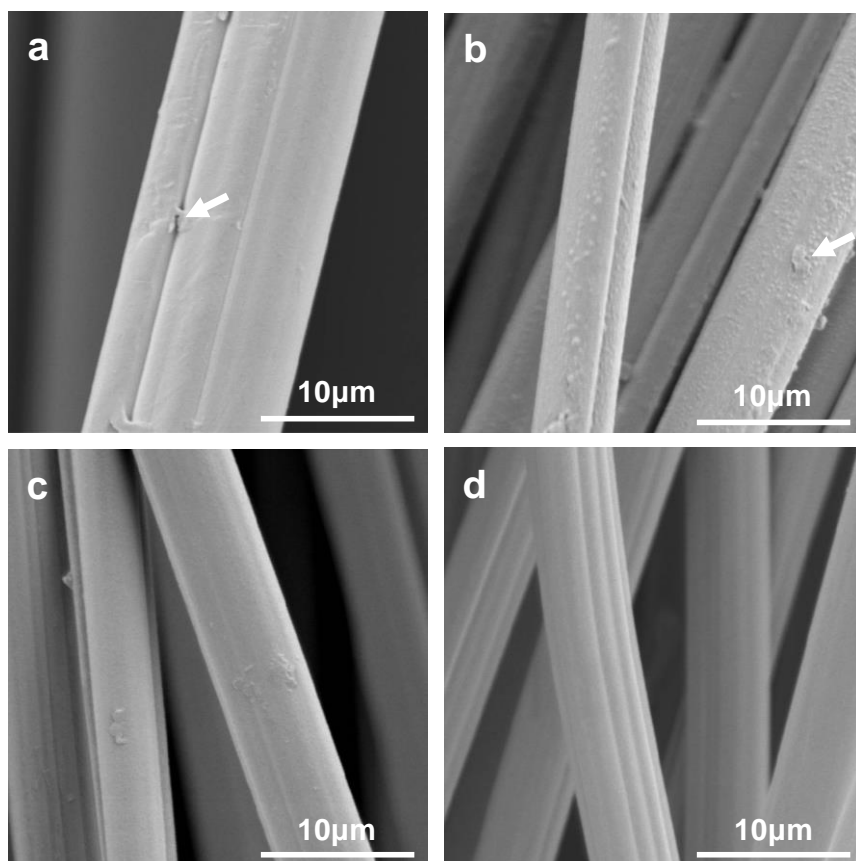


Fig. 3. SEM images of Cordenka 700 fibres (a) and carbonised/graphitised fibres at $1000\text{ }^\circ\text{C}$ (b), $1500\text{ }^\circ\text{C}$ (c) and $2000\text{ }^\circ\text{C}$ (d) at a high magnification. White arrows indicate the presence of defects on the fibre surface.



Fig. 4. Images of the carbon fibre fabrics before and after processing. (a) Before carbonisation, (b) post carbonisation and (c) out of the furnace.

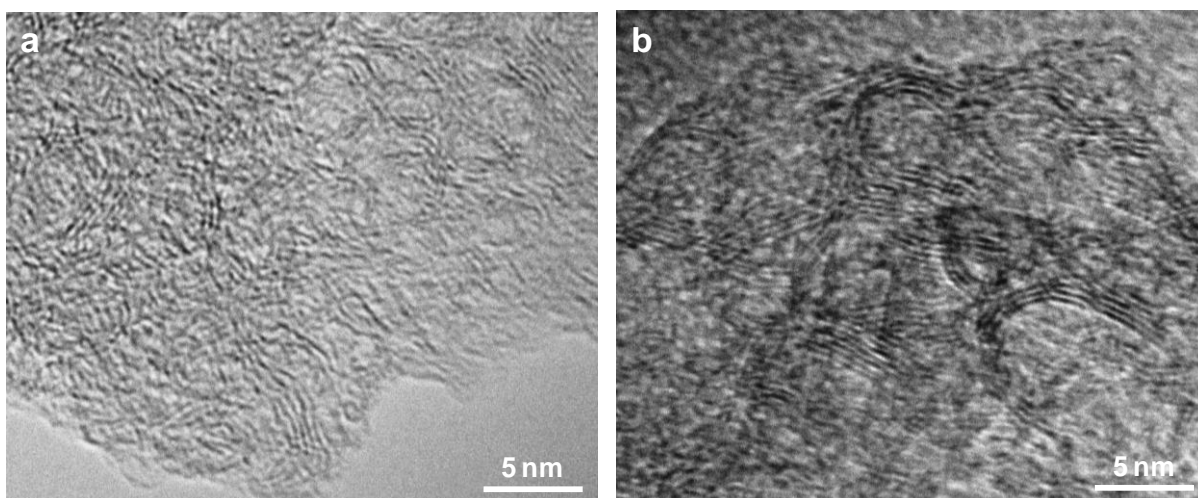


Fig. 5. Typical TEM images of carbon fibres carbonised/graphitised at 1500 °C (a) and 2000 °C (b). Samples were cut for imaging perpendicular to the cross section of the fibres.

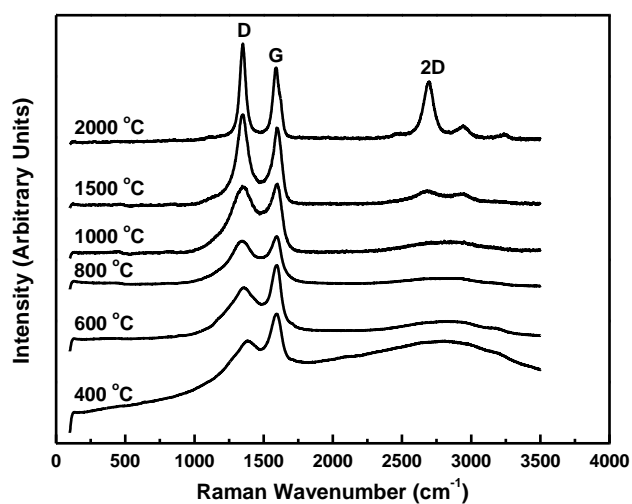
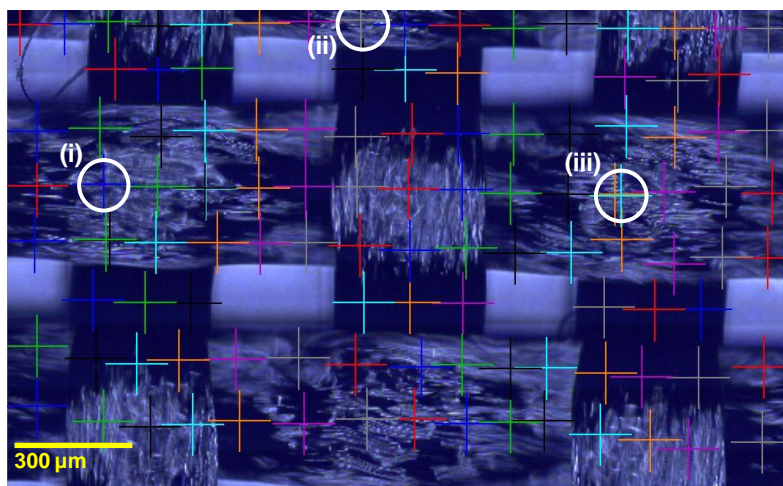


Fig. 6. Typical Raman spectra obtained from Cordenka 700 fibres treated at different temperatures. The positions of the D, G and 2D bands are labelled. The appearance of the 2D Raman band indicates possible graphitisation.

(a)



(b)

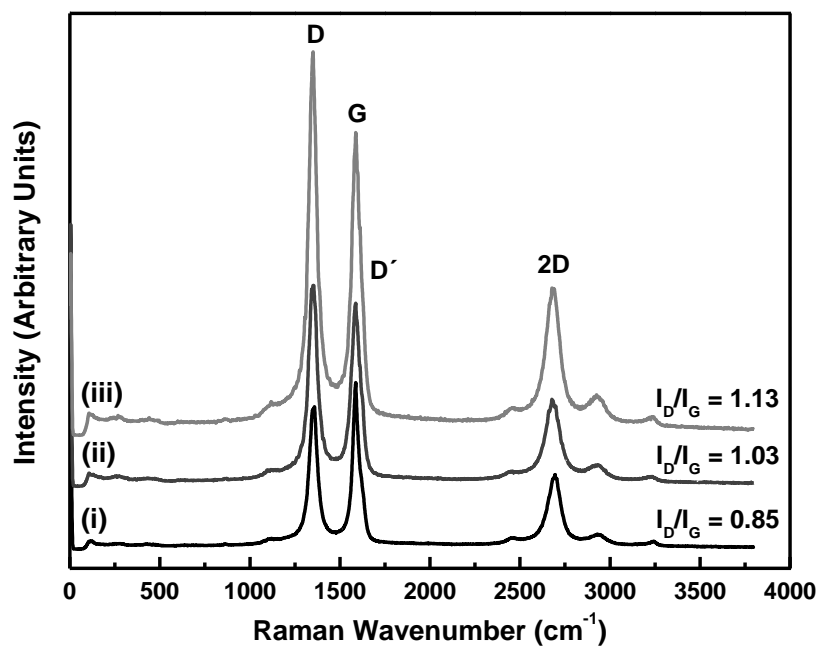
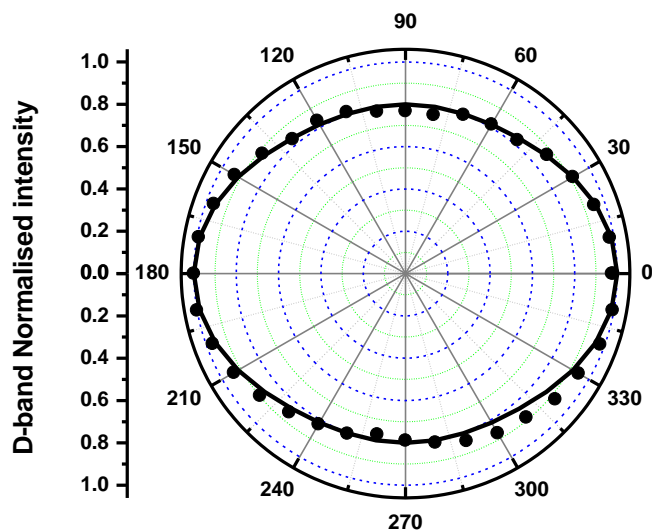


Fig.7. (a) Light microscope image of carbon fibre fabric with regions where Raman spectra recorded (circles – (i) – (iii)) and (b) corresponding Raman spectra (i-iii) recorded from a Cordenka fibre fabric with intensity ratios of the D and G bands (I_D/I_G) - fabrics heated treated at 2000°C (data for 3000°C in Figure S6).

(a)



(b)

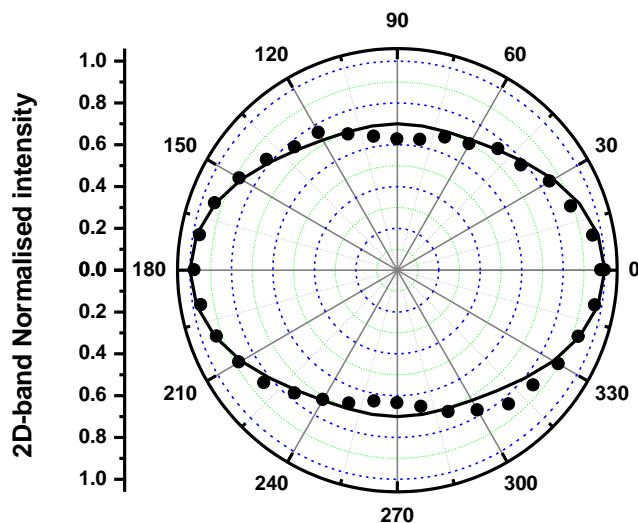
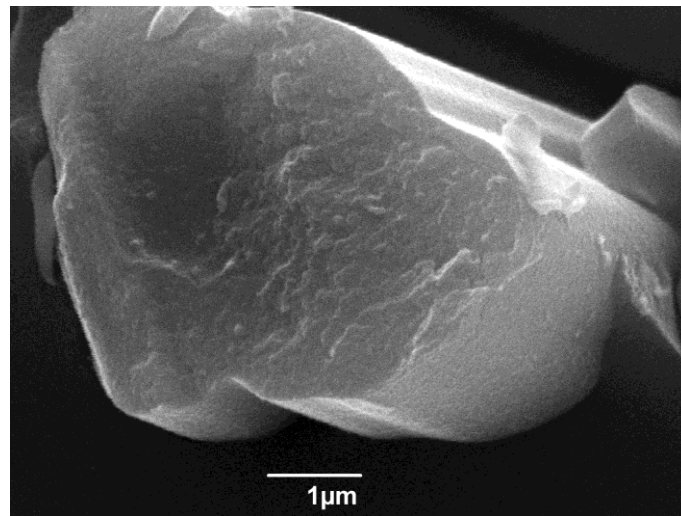


Fig. 8. Normalised intensity of the (a) D and (b) 2D Raman bands as a function of the angle between the polarisation of incident laser direction and the axis of a Cordenka 700-2000 carbonised/graphitised fibre. Solid lines are fits to the data of the form $y = r + t\cos^4\theta$; $r = 0.2$ and $t = 0.8$ in (a) and $r = 0.3$ and $t = 0.7$ in (b). R^2 values for each fit are 0.9.

(a)



(b)

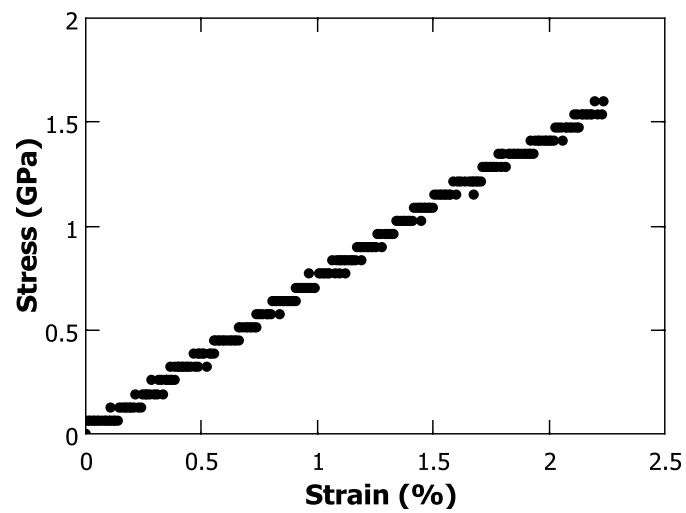
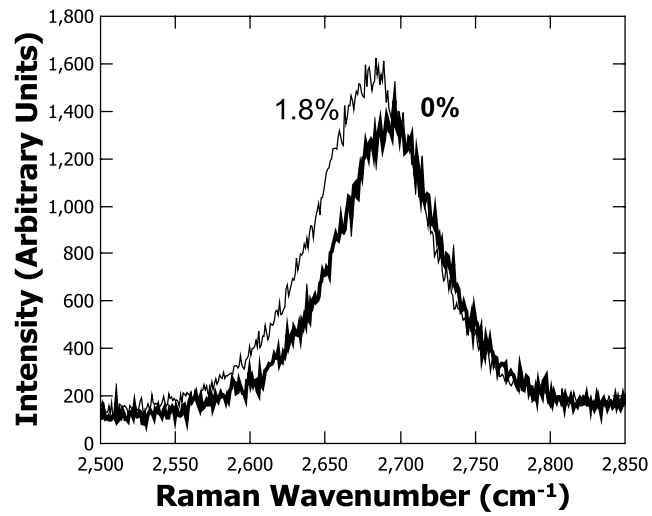


Fig. 9. (a) A typical SEM image of the cross section of a Cordenka 700 fibre carbonised at 2000 °C (Cordenka 700-2000); (b) Typical stress-strain curve of a Cordenka 700-2000 fibre obtained from a DEBEN microtester.

(a)



(b)

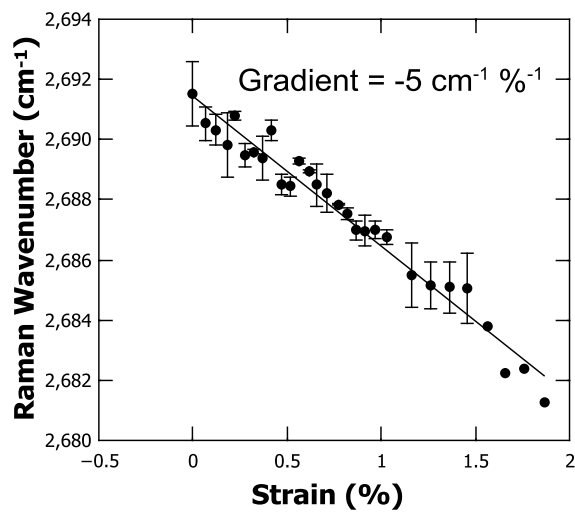


Fig. 10. (a) Shift in the position of the 2D Raman band as a function of strain for a single carbonised/graphitised fibre (Cordenka 700-2000) deformed in tension; (b) detailed shifts in the position of the 2D Raman band initially located at $\sim 2691 \text{ cm}^{-1}$ as a function of tensile deformation. Error bars are for 3 independent fibre tests.